

## **Electronic Supplementary Information**

### **Identification of linear scaling relationships in polysulfide conversion on $\alpha$ -In<sub>2</sub>Se<sub>3</sub> supported single-atom catalysts**

Hui Wang, Lin Zou, Min Li, Long Zhang\*

School of Physics and Electronics, Hunan Key Laboratory of Super Microstructure and Ultrafast Process, Hunan Key Laboratory of Nanophotonics and Devices, State Key Laboratory of Powder Metallurgy, Central South University, Changsha 410083, China

\*E-mail: L.zhang@csu.edu.cn

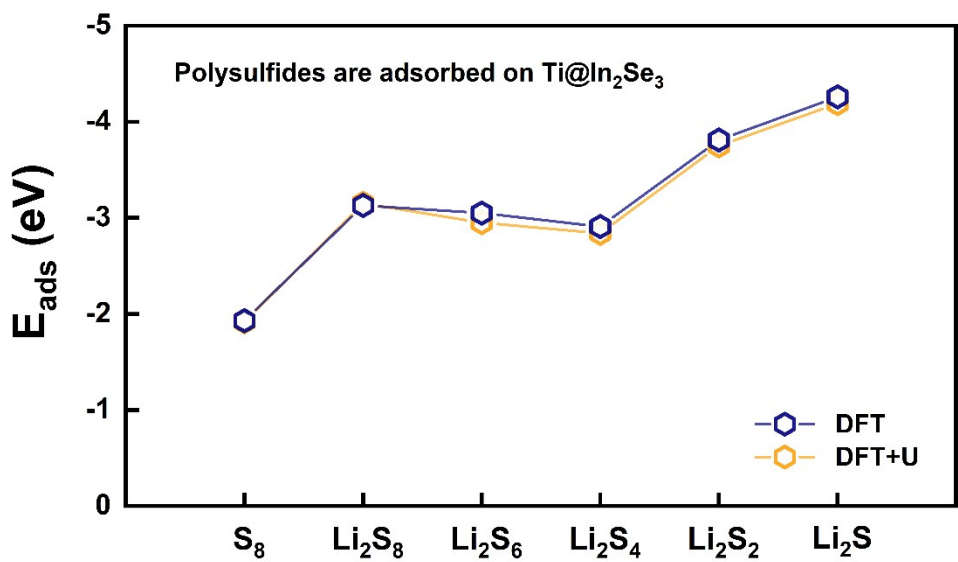


**Fig. S1** Adsorption energies for Li<sub>2</sub>S<sub>n</sub> via DFT and DFT+U ( $U_{\text{eff}} = 2.58$  eV).

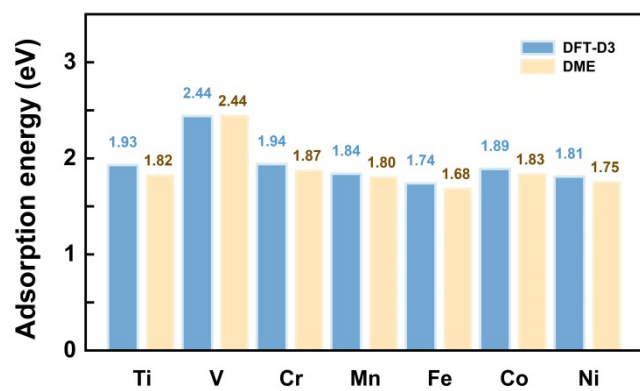


**Fig. S2** Adsorption energies of  $S_8$  with and without consideration of the effect of DME solvent.

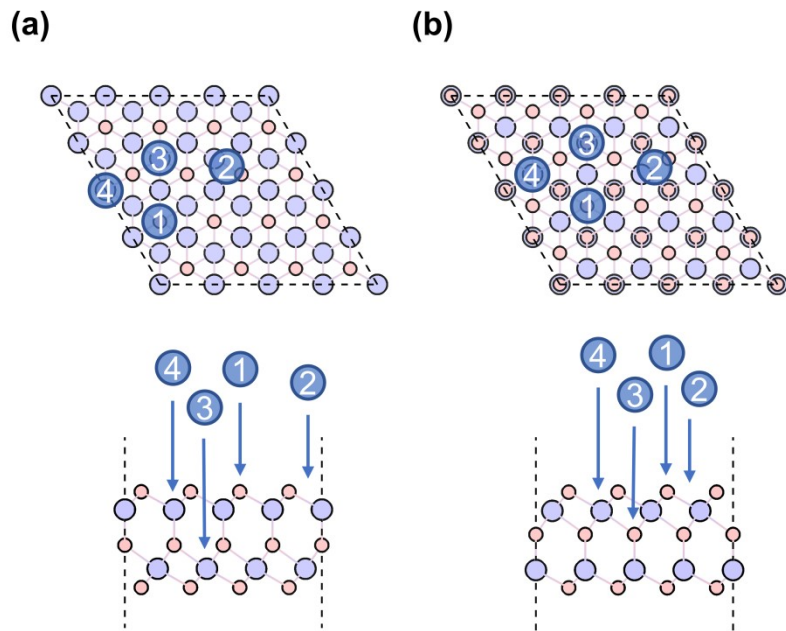


**Fig. S3** Top and side views of (a)  $P_{\uparrow}In_2Se_3$  and (b)  $P_{\downarrow}In_2Se_3$  (color code: pink, Se; purple, In; blue, TM). Four different surface sites, namely, Se top site (site 1), bridge site (site 2), fcc hollow site (site 3), and hcp hollow site (site 4), are labeled.

**Table S1** The values of U parameters for DFT+U calculations (U in eV)

TM	Ti	V	Cr	Mn	Fe	Co	Ni
U	2.58	2.72	2.79	3.06	3.29	3.42	3.40

**Table S2** Binding energies ( $E_b$  in eV) for TM atoms adsorbs on  $P \downarrow In_2Se_3$ 

catalysts	site 1	site 2	site 3	site 4
<b>Ti@In<sub>2</sub>Se<sub>3</sub></b>	-4.98	-5.14	-5.84	-6.35
<b>V@In<sub>2</sub>Se<sub>3</sub></b>	-2.43	-2.52	-4.85	-5.12
<b>Cr@In<sub>2</sub>Se<sub>3</sub></b>	-1.94	-2.14	-3.17	-3.41
<b>Mn@In<sub>2</sub>Se<sub>3</sub></b>	-2.44	-2.45	-3.76	-3.86
<b>Fe@In<sub>2</sub>Se<sub>3</sub></b>	-2.20	-3.10	-4.14	-4.54
<b>Co@In<sub>2</sub>Se<sub>3</sub></b>	-1.95	-1.91	-3.76	-4.28
<b>Ni@In<sub>2</sub>Se<sub>3</sub></b>	-2.55	-2.33	-4.34	-4.73

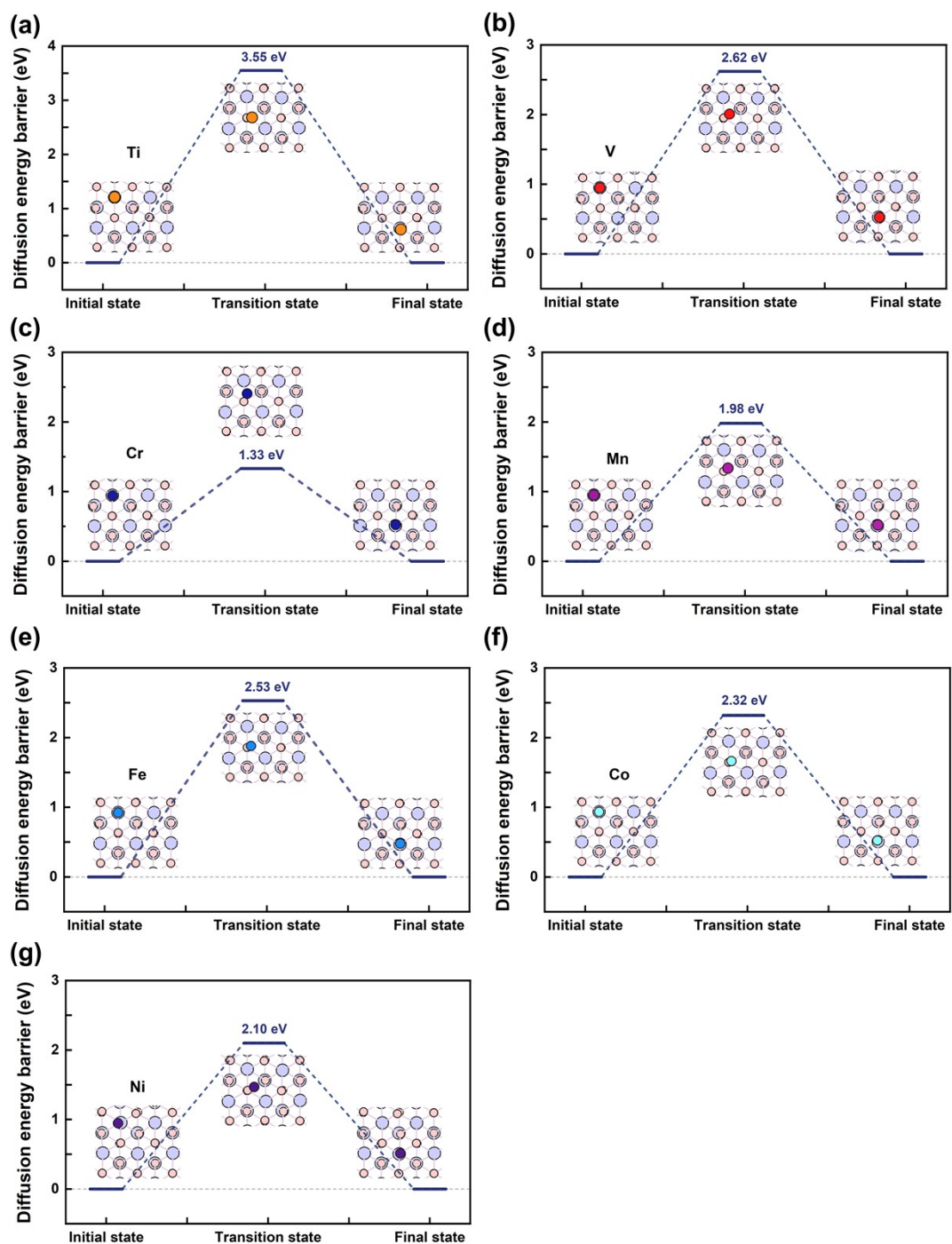


**Fig. S4** Energy profile and corresponding structures for single TM atom diffusion on  $\text{In}_2\text{Se}_3$  surface.

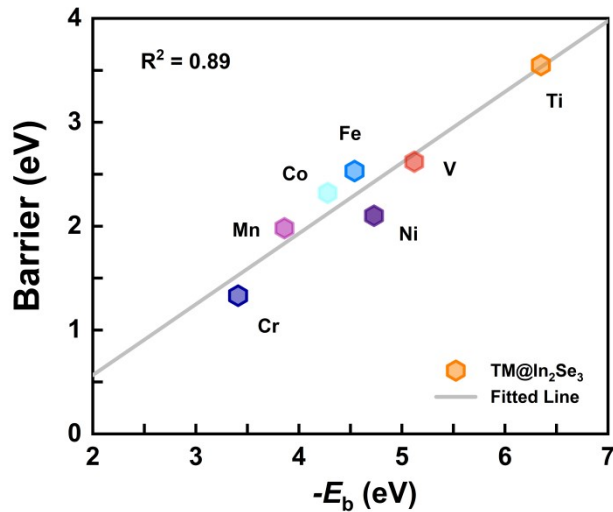


**Fig. S5** Correlation between binding energies ( $E_b$ ) and diffusion barriers (Barrier) for single TM atom absorbed on  $\text{In}_2\text{Se}_3$ .

**Table S3** The binding energies ( $E_b$  in eV) and diffusion barrier (Barrier in eV) for single TM atom on  $\text{In}_2\text{Se}_3$

TM	Ti	V	Cr	Mn	Fe	Co	Ni
$E_b$	-6.35	-5.12	-3.41	-3.86	-4.54	-4.28	-4.73
Barrier	3.55	2.62	1.33	1.98	2.53	2.32	2.10

**Table S4** The average electrons transferred from the anchored TM atoms to the  $\text{In}_2\text{Se}_3$  substrate ( $Q$  in e)

TM	Ti	V	Cr	Mn	Fe	Co	Ni
$Q$	0.88	0.62	0.54	0.63	0.47	0.30	0.03

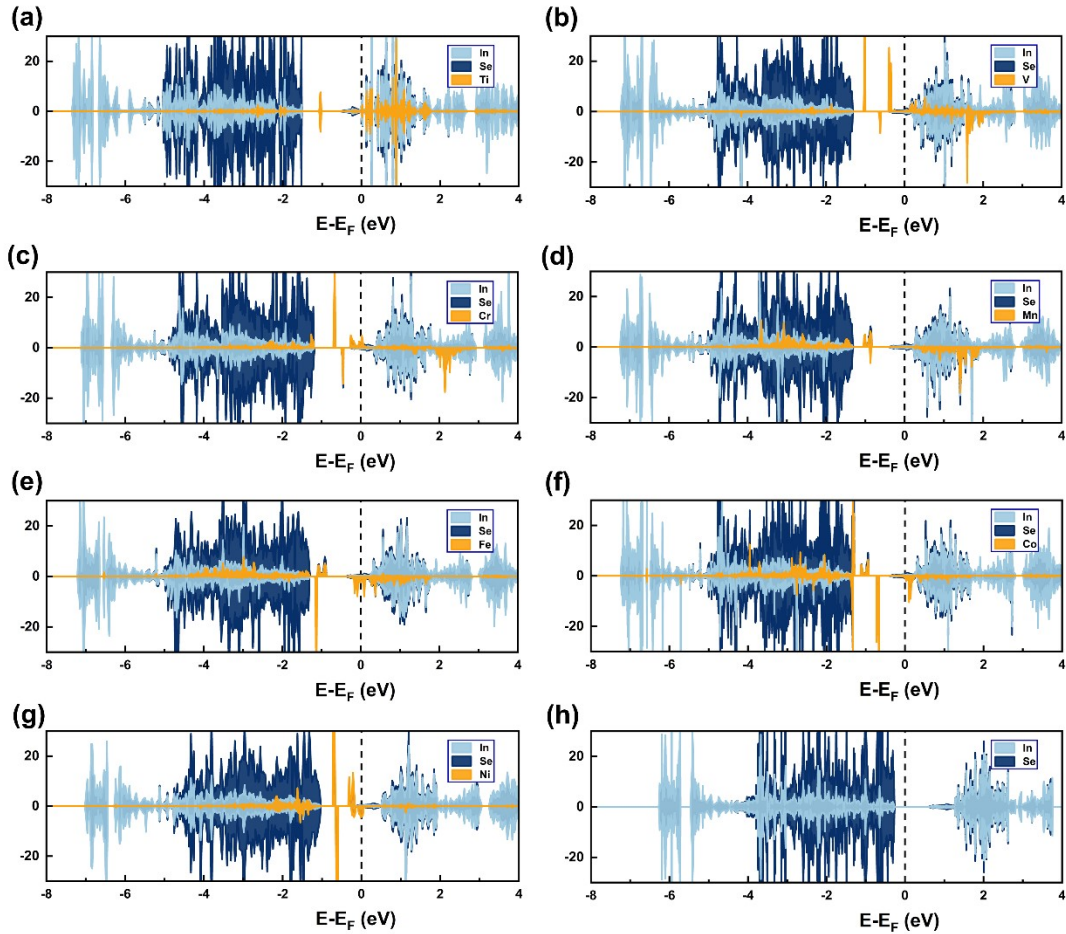


**Fig. S6** Projected density of states (PDOS) of the TM@In<sub>2</sub>Se<sub>3</sub>. (a) Ti@In<sub>2</sub>Se<sub>3</sub>, (b) V@In<sub>2</sub>Se<sub>3</sub>, (c) Cr@In<sub>2</sub>Se<sub>3</sub>, (d) Mn@In<sub>2</sub>Se<sub>3</sub>, (e) Fe@In<sub>2</sub>Se<sub>3</sub>, (f) Co@In<sub>2</sub>Se<sub>3</sub>, (g) Ni@In<sub>2</sub>Se<sub>3</sub>, (h) In<sub>2</sub>Se<sub>3</sub>. The positive and negative values represent the spin-up and spin-down states, respectively. The Fermi level is set to 0 eV.

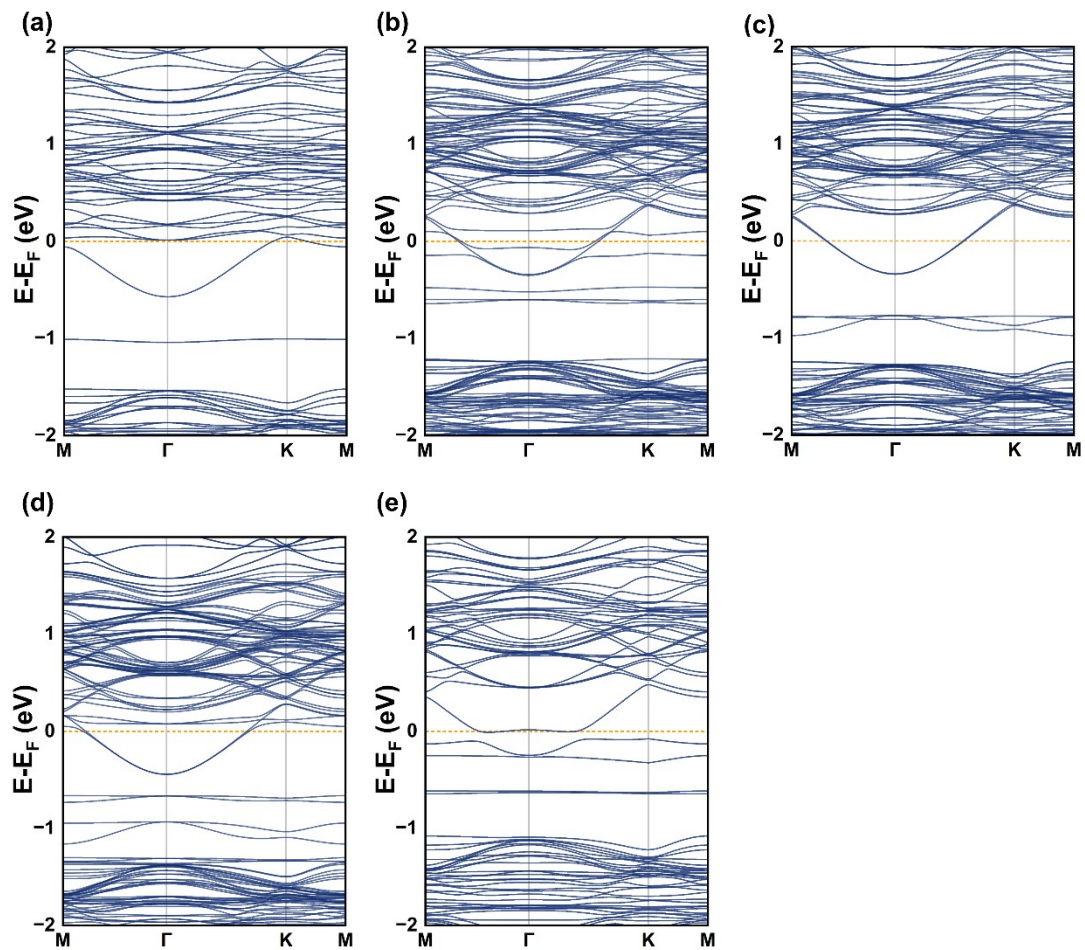


**Fig. S7** Electronic band structures of TM@In<sub>2</sub>Se<sub>3</sub>. (a)-(e) Represent for Ti@In<sub>2</sub>Se<sub>3</sub>, Cr@In<sub>2</sub>Se<sub>3</sub>, Mn@In<sub>2</sub>Se<sub>3</sub>, Co@In<sub>2</sub>Se<sub>3</sub> and Ni@In<sub>2</sub>Se<sub>3</sub>, respectively.

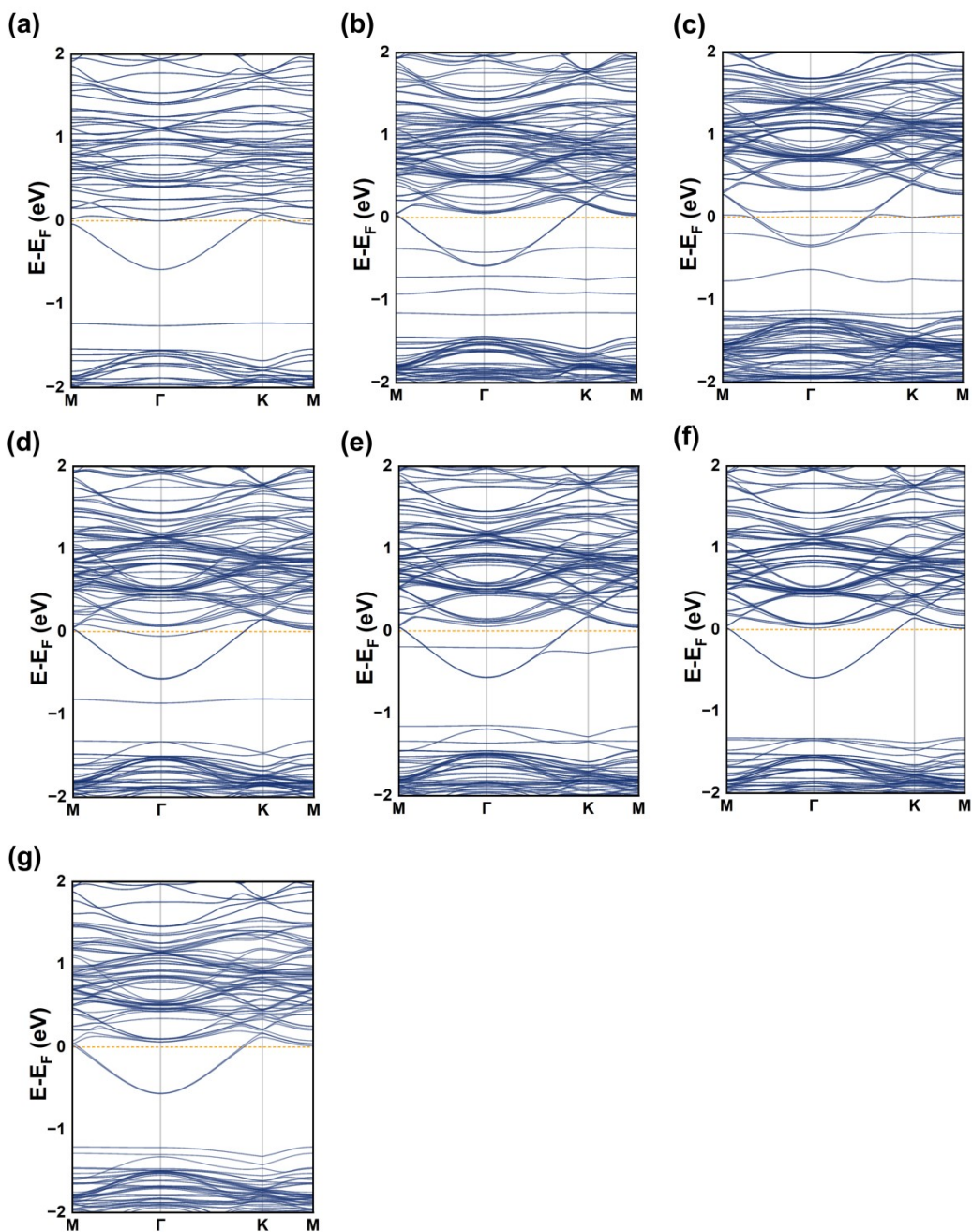


**Fig. S8** Electronic band structures of  $\text{TM}@\text{In}_2\text{Se}_3$  calculated by DFT+U. (a)-(g) Represent for  $\text{Ti}@\text{In}_2\text{Se}_3$ ,  $\text{V}@\text{In}_2\text{Se}_3$ ,  $\text{Cr}@\text{In}_2\text{Se}_3$ ,  $\text{Mn}@\text{In}_2\text{Se}_3$ ,  $\text{Fe}@\text{In}_2\text{Se}_3$ ,  $\text{Co}@\text{In}_2\text{Se}_3$  and  $\text{Ni}@\text{In}_2\text{Se}_3$ , respectively.

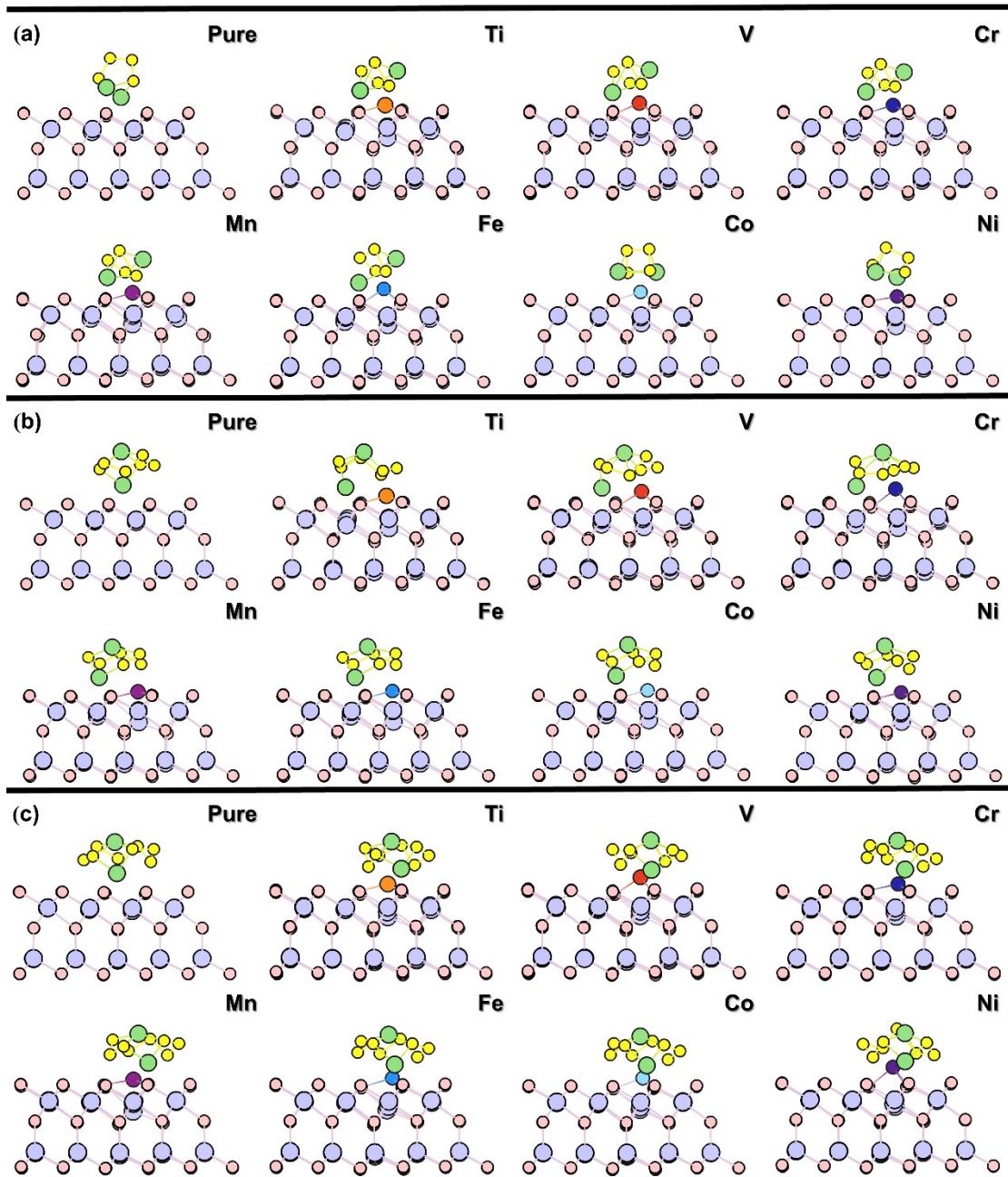


**Fig. S9** Optimized adsorption structures: (a) Li<sub>2</sub>S<sub>4</sub> adsorbs on In<sub>2</sub>Se<sub>3</sub> and TM@In<sub>2</sub>Se<sub>3</sub>, (b) Li<sub>2</sub>S<sub>6</sub> adsorbs on In<sub>2</sub>Se<sub>3</sub> and TM@In<sub>2</sub>Se<sub>3</sub>, (c) Li<sub>2</sub>S<sub>8</sub> adsorbs on In<sub>2</sub>Se<sub>3</sub> and TM@In<sub>2</sub>Se<sub>3</sub> (color code: pink, Se; purple, In; yellow, S; green, Li; other colors, TM)

**Table S5** Adsorption energies for Li<sub>2</sub>S<sub>n</sub> on TM@In<sub>2</sub>Se<sub>3</sub>

Catalyst \ <i>E<sub>ads</sub></i> (eV)	Li <sub>2</sub> S	Li <sub>2</sub> S <sub>2</sub>	Li <sub>2</sub> S <sub>4</sub>	Li <sub>2</sub> S <sub>6</sub>	Li <sub>2</sub> S <sub>8</sub>	S <sub>8</sub>
Catalyst	Li <sub>2</sub> S	Li <sub>2</sub> S <sub>2</sub>	Li <sub>2</sub> S <sub>4</sub>	Li <sub>2</sub> S <sub>6</sub>	Li <sub>2</sub> S <sub>8</sub>	S <sub>8</sub>
In <sub>2</sub> Se <sub>3</sub>	-3.3	-2.33	-1.69	-1.71	-2.19	-1.46
Ti@In <sub>2</sub> Se <sub>3</sub>	-4.26	-3.81	-2.91	-2.85	-3.13	-1.93
V@In <sub>2</sub> Se <sub>3</sub>	-4.36	-3.93	-3.12	-3.29	-3.64	-2.44
Cr@In <sub>2</sub> Se <sub>3</sub>	-4.19	-3.86	-2.81	-2.82	-3.13	-1.94
Mn@In <sub>2</sub> Se <sub>3</sub>	-3.74	-3.2	-2.32	-2.39	-2.79	-1.84
Fe@In <sub>2</sub> Se <sub>3</sub>	-3.53	-2.89	-2.23	-2.27	-2.63	-1.74
Co@In <sub>2</sub> Se <sub>3</sub>	-3.59	-3.19	-2.34	-2.37	-2.81	-1.89
Ni@In <sub>2</sub> Se <sub>3</sub>	-3.38	-2.87	-2.39	-2.29	-2.8	-1.81

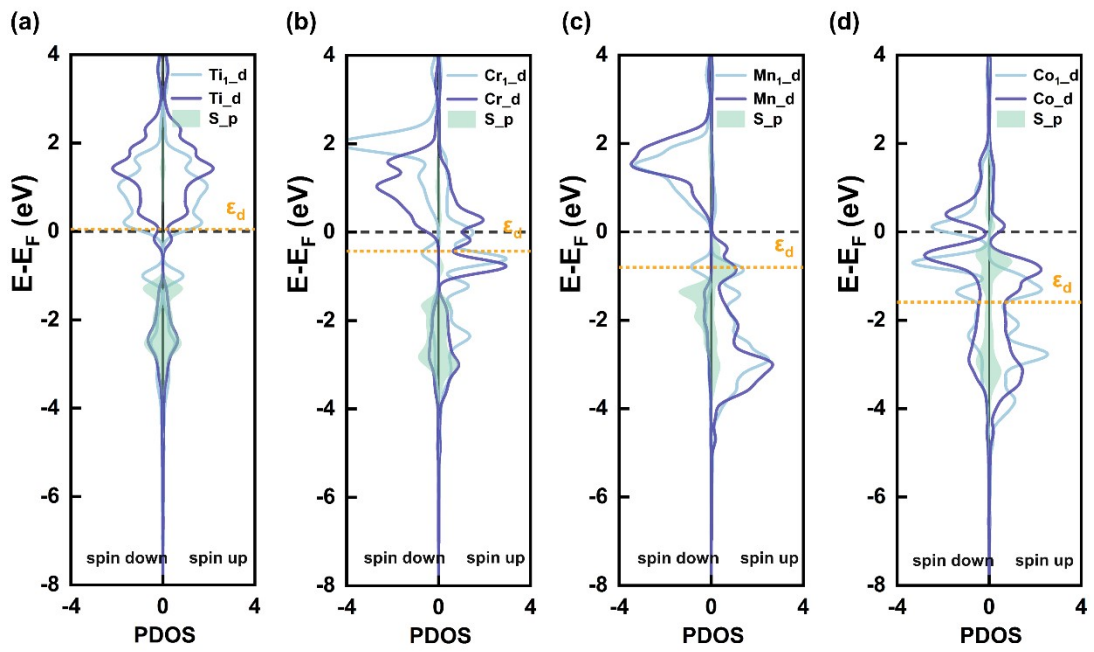


**Fig. S10** (a)-(d) Projected density of states (PDOS) for  $\text{Li}_2\text{S}$  adsorbed on  $\text{Ti}@\text{In}_2\text{Se}_3$ ,  $\text{Cr}@\text{In}_2\text{Se}_3$ ,  $\text{Mn}@\text{In}_2\text{Se}_3$ , and  $\text{Co}@\text{In}_2\text{Se}_3$ , respectively.

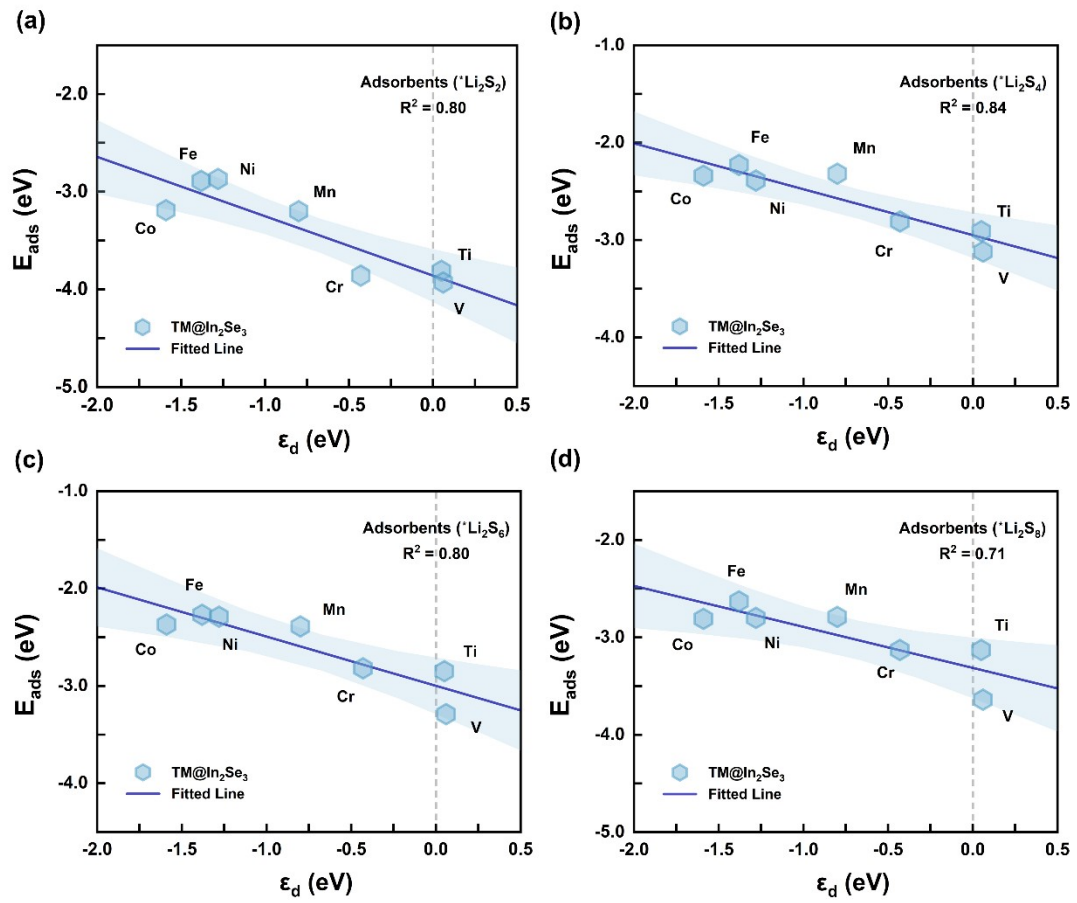


**Fig. S11** (a)-(d) The correlation between  $\epsilon_d$  of the adsorbed TM atoms and  $E_{\text{ads}}$  for  $\text{Li}_2\text{S}_2$ ,  $\text{Li}_2\text{S}_4$ ,  $\text{Li}_2\text{S}_6$ , and  $\text{Li}_2\text{S}_8$  adsorption.

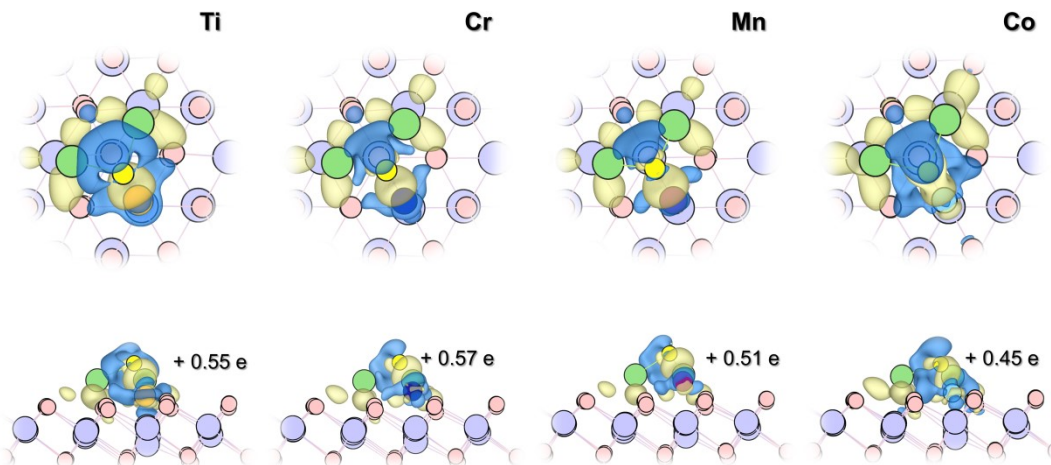


**Fig. S12** Top view and side view of charge density differences for  $\text{Li}_2\text{S}$  adsorbed on  $\text{Ti}@\text{In}_2\text{Se}_3$ ,  $\text{Cr}@\text{In}_2\text{Se}_3$ ,  $\text{Mn}@\text{In}_2\text{Se}_3$ , and  $\text{Co}@\text{In}_2\text{Se}_3$ . Yellow and blue states represent the charge accumulation and loss, respectively. The isosurface is set to be  $0.003 \text{ e}/\text{bohr}^3$ . The amount of charge accumulated on S of the adsorbed  $\text{Li}_2\text{S}$  is presented.

**Table S6** The average Li-S bond length ( $d_{\text{Li-S}}$  in Å) and S-S bond length ( $d_{\text{S-S}}$  in Å) for  $\text{Li}_2\text{S}_2$  absorbed on  $\text{In}_2\text{Se}_3$  and TM@ $\text{In}_2\text{Se}_3$

<b>TM</b>	<b>Pure</b>	<b>Ti</b>	<b>V</b>	<b>Cr</b>	<b>Mn</b>	<b>Fe</b>	<b>Co</b>	<b>Ni</b>
$d_{\text{Li-S}}$	2.39	2.48	2.48	2.49	2.52	2.51	2.50	2.51
$d_{\text{S-S}}$	2.05	2.09	2.08	2.06	2.05	2.04	2.03	2.03

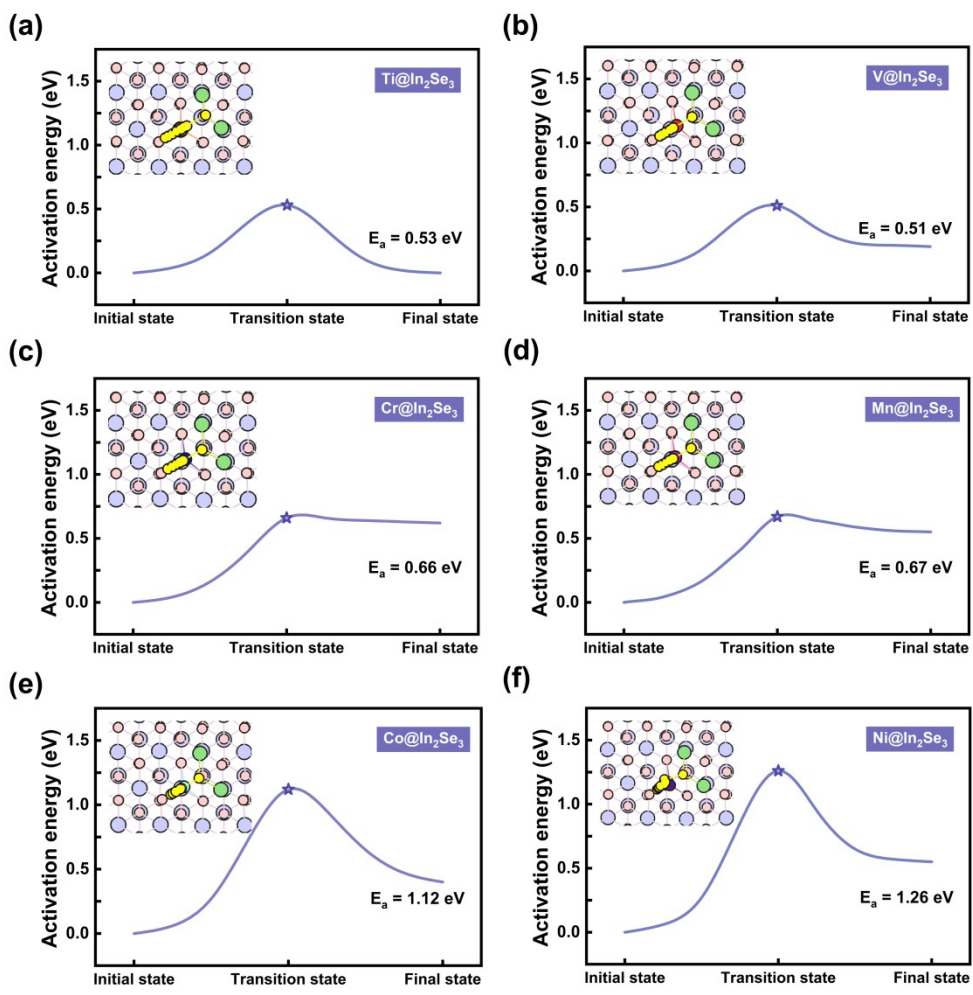


**Fig. S13** (a)-(f) Energy profiles and corresponding structures for Li<sub>2</sub>S<sub>2</sub> dissociation on Ti@In<sub>2</sub>Se<sub>3</sub>, V@In<sub>2</sub>Se<sub>3</sub>, Cr@In<sub>2</sub>Se<sub>3</sub>, Mn@In<sub>2</sub>Se<sub>3</sub>, Co@In<sub>2</sub>Se<sub>3</sub>, and Ni@In<sub>2</sub>Se<sub>3</sub>.

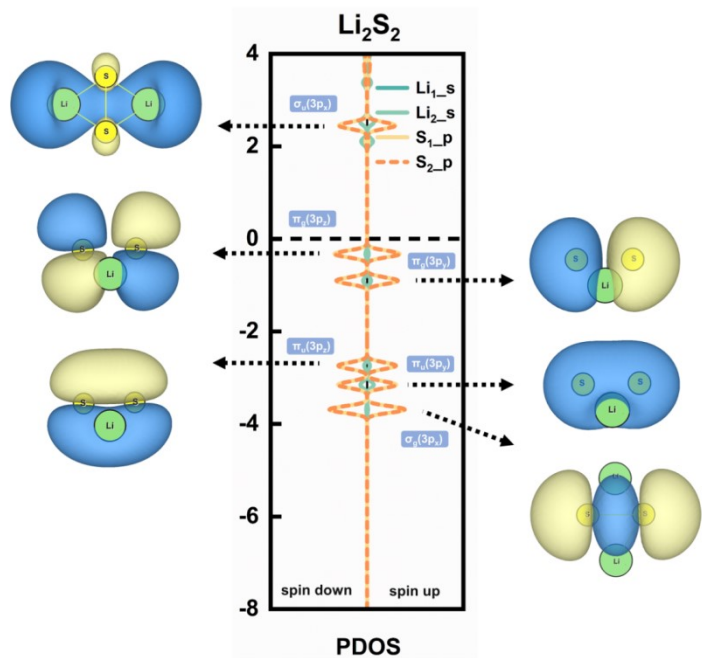


**Fig. S14** Molecular orbitals of gas-phase  $\text{Li}_2\text{S}_2$ .

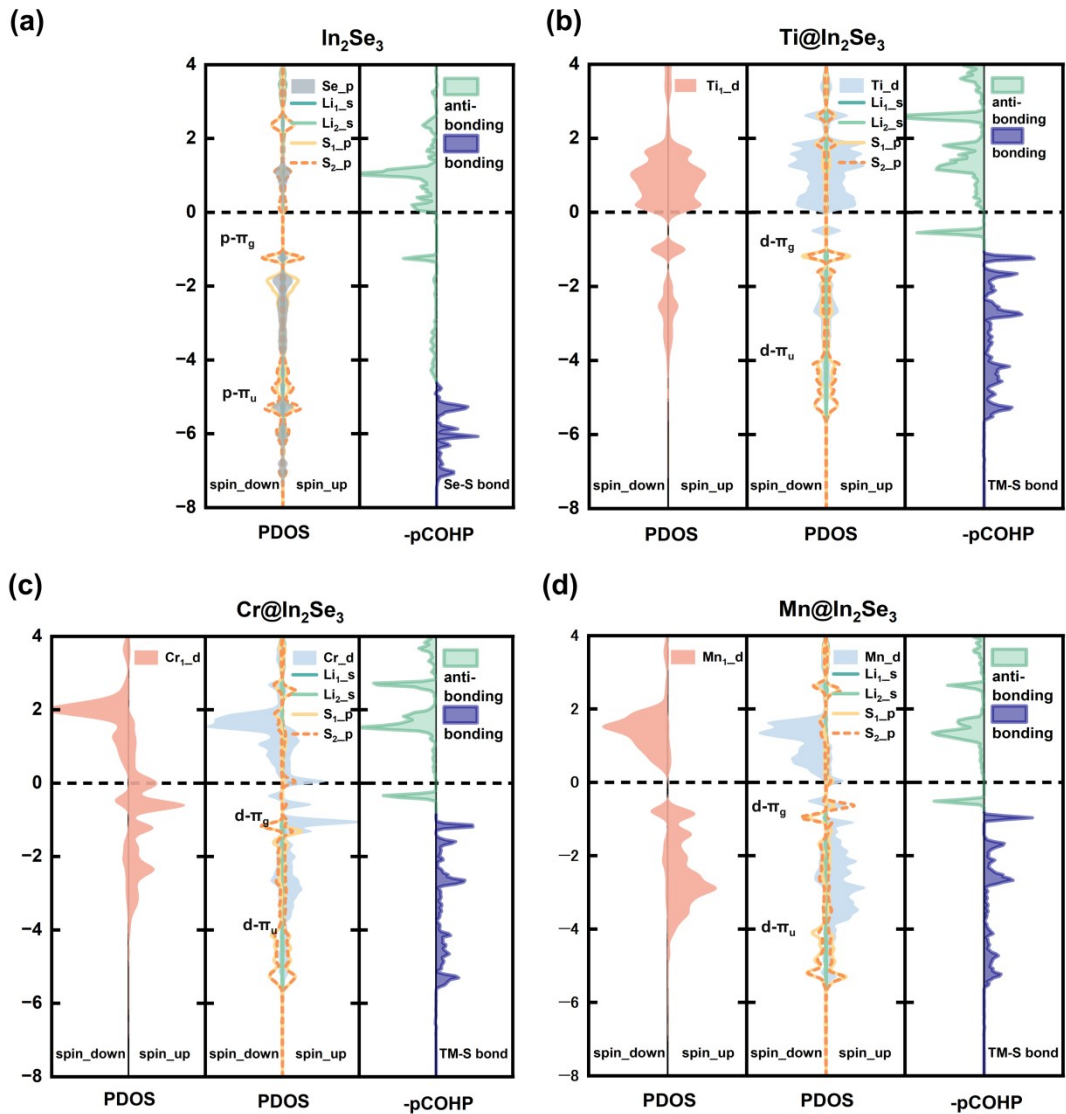


**Fig. S15** Projected density of states (PDOS) and projected crystal orbital Hamilton population (pCOHP) for  $\text{Li}_2\text{S}_2$  adsorbed on (a)  $\text{In}_2\text{Se}_3$ , (b)  $\text{Ti}@\text{In}_2\text{Se}_3$ , (c)  $\text{Cr}@\text{In}_2\text{Se}_3$ , (d)  $\text{Mn}@\text{In}_2\text{Se}_3$ .

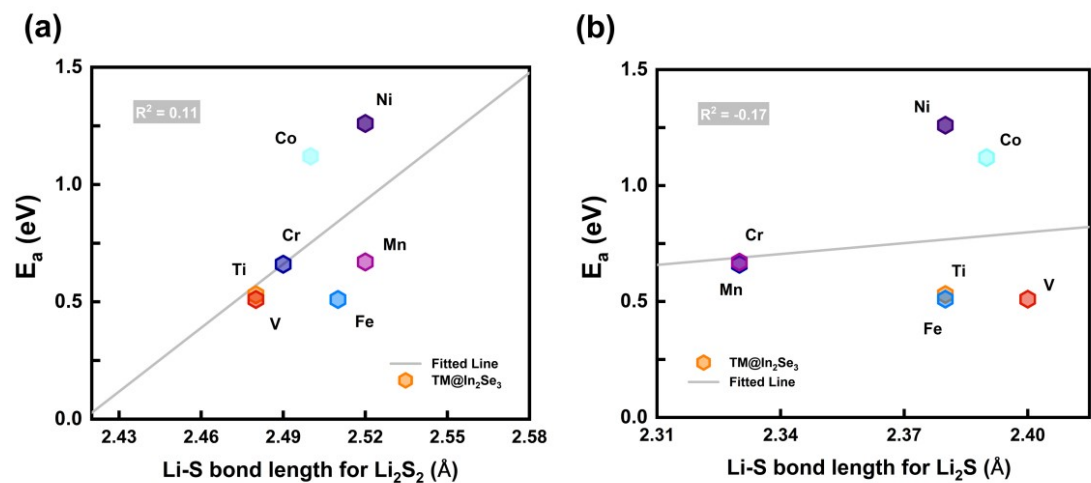


**Fig. S16** Correlation between activation energy and Li-S bond length for (a) the adsorbed  $\text{Li}_2\text{S}_2$  and the adsorbed  $\text{Li}_2\text{S}$ .